

High-yield magnetic recoil neutron spectrometer on the National Ignition Facility for operation up to 60 MJ

Cite as: Rev. Sci. Instrum. **93**, 083513 (2022); <https://doi.org/10.1063/5.0099317>

Submitted: 16 May 2022 • Accepted: 27 June 2022 • Published Online: 17 August 2022

 M. Gatu Johnson,  T. M. Johnson,  B. J. Lahmann, et al.

COLLECTIONS

Paper published as part of the special topic on [Proceedings of the 24th Topical Conference on High-Temperature Plasma Diagnostics](#)



View Online



Export Citation



CrossMark

Lock-in Amplifiers
up to 600 MHz



Zurich
Instruments



High-yield magnetic recoil neutron spectrometer on the National Ignition Facility for operation up to 60 MJ

Cite as: Rev. Sci. Instrum. 93, 083513 (2022); doi: 10.1063/5.0099317

Submitted: 16 May 2022 • Accepted: 27 June 2022 •

Published Online: 17 August 2022



View Online



Export Citation



CrossMark

M. Gatu Johnson,^{1,a)} T. M. Johnson,¹ B. J. Lahmann,¹ F. H. Séguin,¹ B. Sperry,¹ N. Bhandarkar,² R. M. Bionta,² E. Casco,² D. T. Casey,² A. J. Mackinnon,² N. Masters,² A. Moore,² A. Nikroo,² M. Hoppe,³ R. Mohammed,³ W. Sweet,³ C. Freeman,⁴ V. Picciotto,⁴ J. Roumell,⁴ and J. A. Frenje¹

AFFILIATIONS

¹Massachusetts Institute of Technology, Cambridge, Massachusetts 02139, USA

²Lawrence Livermore National Laboratory, Livermore, California 94550, USA

³General Atomics, San Diego, California 92186, USA

⁴State University of New York at Geneseo, Geneseo, New York 14454, USA

Note: This paper is part of the Special Topic on Proceedings of the 24th Topical Conference on High-Temperature Plasma Diagnostics.

^{a)} Author to whom correspondence should be addressed: gatu@psfc.mit.edu

ABSTRACT

Recent progress at the National Ignition Facility (NIF), with neutron yields of order 1×10^{17} , places new constraints on diagnostics used to characterize implosion performance. The Magnetic Recoil neutron Spectrometer (MRS), which is routinely used to measure yield, ion temperature (T_{ion}), and down-scatter ratio (d_{sr}), has been adapted to allow measurements of d_{sr} up to 5×10^{17} , and yield and T_{ion} up to 2×10^{18} in the near term with new data processing techniques and conversion foil solutions. This paper presents a solution for extending MRS operation up to a yield of 2×10^{19} (60 MJ) by moving the spectrometer outside of the NIF shield wall. This will not only enhance the upper yield limit by $10\times$ but also improve signal-to-background by $5\times$.

Published under an exclusive license by AIP Publishing. <https://doi.org/10.1063/5.0099317>

I. INTRODUCTION

Yields from cryogenically layered deuterium–tritium (DT) inertial confinement fusion (ICF) implosions at the National Ignition Facility (NIF) are reaching new records of order 1×10^{17} ,¹ ushering in an era of unprecedented opportunities and challenges for the instruments used to diagnose ICF plasmas. NIF neutron spectrometers are used to provide² the critical performance parameters of neutron yield, ion temperature (T_{ion} , inferred from the width of the primary 14 MeV neutron spectrum^{3–5}), and areal density (through the downscatter ratio, d_{sr} , calculated⁶ as the ratio of the neutron yield in the energy ranges from 10–12 to 13–15 MeV).

One of the NIF neutron spectrometers is the magnetic recoil neutron spectrometer (MRS; Fig. 1).^{7,8} Prior to the recent record experiments, MRS allowed operation up to a ceiling yield of

$\sim 9 \times 10^{16}$. This paper discusses how adapting CR-39 processing and analysis techniques (Sec. II) and using smaller foils (Sec. III) have allowed an increase in this ceiling to 2×10^{18} in the short term. Two different foil configurations are considered: a stand-alone foil at 26 cm from the implosion and a glow-discharge-polymer deposited foil fielded on the hohlraum for significantly improved resolution.^{9,10} For the hohlraum foils, challenges due to uncontrolled foil motion, foil oxygen uptake, and background n,d reactions are discussed, and potential solutions are proposed. The smaller foils come with reduced efficiency detrimentally impacting signal-to-background (S/B).¹¹ In the current configuration, MRS d_{sr} data are likely to be compromised at yields $> 5 \times 10^{17}$. This paper also proposes a solution to this problem: moving the MRS behind the outer NIF shield wall (Sec. IV). Monte Carlo n-particle (MCNP) simulations predict an increase in the d_{sr} yield limit to $\sim 2 \times 10^{19}$ for this proposed configuration.

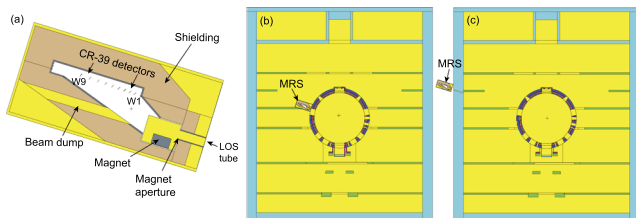


FIG. 1. (a) MCNP model of the NIF MRS with the detector components indicated, (b) in its current location on the NIF target chamber, and (c) in its proposed new location outside of the shield wall.

II. OPERATION LIMITS OF THE CURRENT NIF MRS

The MRS consists of a deuterated plastic (CD) foil positioned close to the implosion, a permanent Nd-Fe-B magnet behind a fixed-size aperture outside of the target chamber wall, and an array of CR-39 detectors in the magnet focal plane. A fraction of the neutrons from an ICF implosion scatter elastically in the CD foil, generating recoil deuterons, which are subsequently momentum separated in the magnet to end up in a different physical location on the detector array depending on their energy. The neutron spectrum is inferred from the measured recoil deuteron energy spectrum using a response function calculated based on the well-known n,d elastic scattering cross section and the geometry of the setup. The MRS setup can be adapted to the predicted yield of an experiment by changing the CD foil;⁵ the current lowest efficiency/highest resolution configuration available is a 50- μm thick, 3 cm^2 active area foil giving an efficiency of 4.4×10^{-12} deuteron tracks/source neutron and an FWHM resolution of 0.43 MeV (henceforth referred to as the “high yield configuration”).

The upper yield limit for MRS operation depends on the density of tracks on the CR-39 coupons used in the detector array.¹² At the nominal 6 h etch time, a rule-of-thumb is that the track density should be $<1.5 \times 10^4 \text{ cm}^{-2}$. As the track overlap limit scales with the square of the track size,¹² which in turn scales with etch time,¹³ this upper limit can be increased by reducing the etch time of the CR-39 coupons. For the exposure and etch conditions of the NIF MRS CR-39, it is found that a minimum etch time of 1.25 h is required for all signal tracks to develop. A small amount of track overlap can be corrected in the analysis by identifying ellipsoidal tracks that are likely to represent overlapping tracks and double-counting these tracks. Using the two methods of short etch time and overlap correction combined, the MRS has been successfully operated up to a track density of $5 \times 10^5 \text{ cm}^{-2}$, corresponding to a neutron yield limit of $\sim 5 \times 10^{17}$ in the standard high yield configuration (the average track diameter in the primary peak for NIF MRS at 6 h etch is 8.2 μm , and at 1.25 h etch is 2.3 μm).

A. Background considerations

Two types of background must be considered when analyzing NIF MRS data: intrinsic (due to CR-39 defects) and neutron-induced (due to neutrons knocking out charged particles in the CR-39). The intrinsic background varies significantly between pieces

of CR-39 and with analysis conditions, particularly the darkness (i.e., contrast) of the tracks considered in the analysis.¹⁴ An average value at contrast $c < 13\%$ is $199 \pm 165 \text{ cm}^{-2}$, with the large 1σ error bar capturing the substantial piece-to-piece variations observed. The average increases to 942 at $c < 35\%$ and 6930 at $c < 65\%$. The neutron-induced background also varies with analysis conditions and additionally with neutron energy and etch time. The typical CR-39 neutron detection efficiencies at 6 h etch for $c < 35\%$ and eccentricity $e < 35\%$ are $(6.0 \pm 0.7) \times 10^{-5}$ per incident neutron for 14 MeV DT neutrons and $(1.1 \pm 0.2) \times 10^{-4}$ per incident neutron for 2.5 MeV DD neutrons.¹⁵ To allow determination of the expected neutron background in the NIF MRS data, the neutron fluence per source neutron on the MRS detector is calculated using the MCNP code,¹⁶ with the model shown in Fig. 1 and the result shown in Fig. 2. As an example of the expected balance of intrinsic vs neutron-induced background and as a check of the validity of the MCNP model, consider the MRS data measured on CR-39 detector No. 8 from NIF experiment N210808, etched for 6 h. The total analyzed area on this piece of CR-39 is 28 cm^2 . A total of 4005 signal tracks are isolated by (i) limiting the accepted tracks to $c < 13\%$, $e < 15\%$, and diameter $7 < d < 10.2 \mu\text{m}$ and (ii) subtracting a uniform background, inferred from the observed tracks in the background region (which could be intrinsic or neutron-induced), scaled up to the full piece, of 38 900 tracks. With this CR-39 area and contrast limit, the expected intrinsic background level is ~ 5600 tracks, and thus a factor 7 lower than the neutron-induced background in this particular case. With the simulated background neutron fluence of

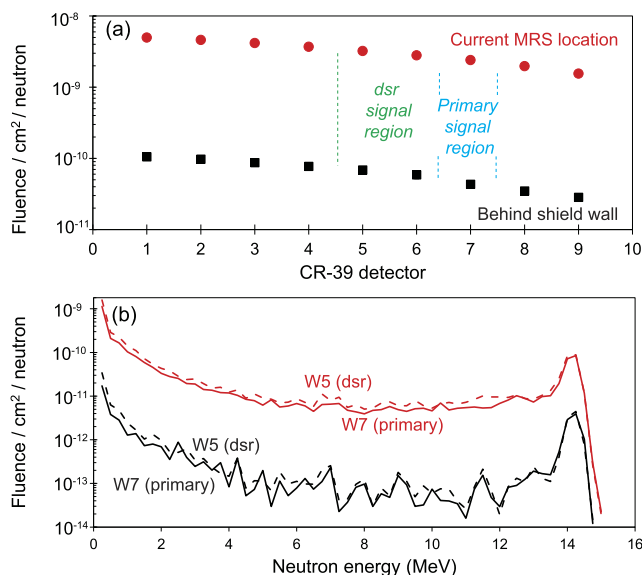


FIG. 2. (a) MCNP-calculated neutron background fluence per produced neutron on each CR-39 piece in the MRS detector, for the current configuration (red circles) and the proposed location outside of the NIF shield wall (black squares). The error bars are smaller than the symbols. (b) MCNP-simulated neutron background spectra for the primary detector (W7, solid lines) and the dsr detector (W5, dashed lines), again with the current configuration in red and the proposed outside-of-shield-wall configuration in black.

1.3×10^{-9} on W8 (Fig. 2), the yield on this shot of 4.54×10^{17} , and the expected CR-39 efficiency for DT neutrons of 6×10^{-5} , the predicted neutron background at $c < 35\%$ and $e < 35\%$ is $\sim 1 \times 10^6$. While this is substantially higher than the 3.3×10^4 inferred for the tighter track diameter bounds used above, if the c and e limits in the analysis are both relaxed to 35%, a total background of 1.4×10^6 is, instead, found on this detector. Considering that the CR-39 neutron detection efficiency increases with decreasing neutron energy and that the average neutron energy is well below 14 MeV [Fig. 2(b)], this roughly agrees with the prediction, with the data supporting the validity of the MCNP result.

As discussed in Ref. 11, any background, which is uniform across the CR-39, can be straightforwardly subtracted in the analysis of the data on each individual CR-39 detector. However, the neutron-induced background across the CR-39 in the d_{sr} region of the MRS spectrum in the current configuration is found to be non-uniform. This background was measured on two shots, N130628 and N151020, with MRS fielded without a CD conversion foil and with neutron yields of 1.6×10^{15} and 3.5×10^{15} , respectively [Fig. 3(a)]. MRS data are corrected for this by scaling the empirically measured background by the neutron yield on each new shot and subtracting before inferring a d_{sr} number, as shown in Fig. 3(b). It should be noted that at the recent high yield levels, this background is extrapolated by two orders of magnitude, raising questions about the accuracy of features of the component, particularly the fall-off and shape of its high-energy tail, which was at the noise level at 3.5×10^{15} yield. Background data should be obtained at a higher yield in the near term to check this. The 10–12 MeV neutron energy

range of interest in the d_{sr} calculation approximately corresponds to 8.9–10.7 MeV deuteron energy (E_d). As can be seen in Fig. 3(b), the ratio of the non-uniform neutron background (green triangles) to signal (blue diamonds) in this energy range varies from $\sim 1:1$ to 4:1. Reducing MRS efficiency without also improving S/B will linearly drop the signal while keeping the background the same; such efficiency reduction will clearly compromise the d_{sr} measurement. Given this constraint, the d_{sr} upper yield limit for the current MRS is estimated to be 5×10^{17} .

Given that the background scales directly with neutron yield, there will also be an upper yield limit where MRS data saturates on neutron background alone. Assuming a maximum acceptable track density of $5 \times 10^5 \text{ cm}^{-2}$ and a total CR-39 neutron detection efficiency of 6×10^{-5} , this limit for the primary data on W7 will be $\sim 3.5 \times 10^{18}$.

The other new consideration impacting MRS analysis at yields $> 1 \times 10^{17}$ is that the coincidence counting technique¹⁷ (CCT) previously used to eliminate intrinsic background and reduce neutron-induced background in the MRS analysis fails. The reason for this is that the number of random coincidences scales with track density squared; at 1×10^{17} yield, the track density on MRS becomes high enough where the CCT background overtakes the background inferred from standard, front side CR-39 counting (SCT). The use of SCT means that the analysis becomes susceptible to gradients in the intrinsic background, which now has to be subtracted assuming it is uniform across the piece. A comparison of CCT and SCT analysis over a range of implosions has been undertaken to verify that the two methods agree on average, while the SCT results scatter up and down around the established CCT result, depending on the shot. This is concluded to result from variations in intrinsic noise gradients and leads to larger uncertainty in the d_{sr} numbers inferred from SCT than from CCT analysis.

III. REDUCING EFFICIENCY I: THE FOIL METHOD

A short-term solution for avoiding saturation at high yield is to reduce the MRS efficiency by reducing the number of deuterons available for n,d scattering in the foil. As discussed above, this will quickly lead to an S/B problem in the d_{sr} measurement, but it will facilitate primary yield and T_{ion} measurements up to a higher upper yield limit than previously possible. With MRS expected to saturate on background alone at $\sim 3.5 \times 10^{18}$ as discussed above, it is reasonable to aim for an upper yield limit of 2×10^{18} when designing the new foil configuration.

As discussed in Ref. 5, two methods exist for manufacturing MRS foils: (i) the hot-press method, which can be used to make stand-alone CD_2 foils down to $50 \mu\text{m}$ thickness, and (ii) the glow discharge polymer deposition (GDP) method, which can be used to make arbitrarily thin foils. The GDP foils have been found to degrade rapidly with time when used on more than one shot and also to delaminate from the backer they are deposited onto, and thus, they are not feasible for repeated use. Hence, the standard MRS foils fielded at 26 cm from the implosions are all made using the hot-press method. Since the MRS already uses the minimum thickness available for this foil type, the path forward to reduced efficiency is to reduce the foil area. The easiest way to achieve this

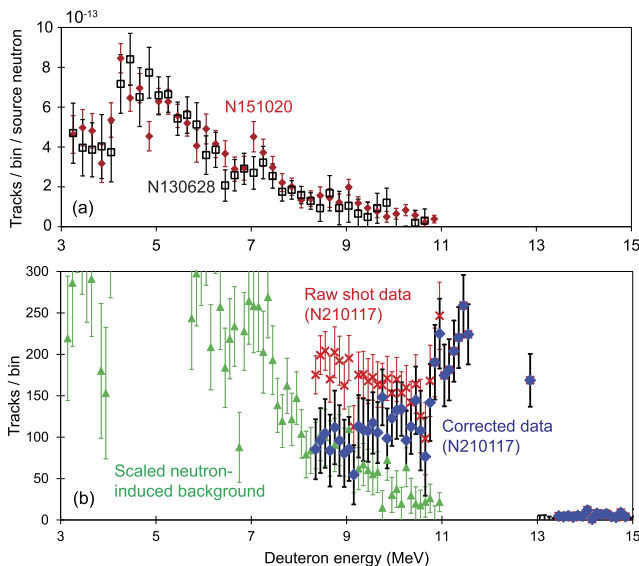


FIG. 3. (a) Non-uniform neutron-induced background, normalized by the neutron yield, measured on two shots with MRS fielded without a CD conversion foil: N130628 and N151020. The results from the two shots are seen to track each other closely. (b) MRS data from shot N210117, with MRS fielded in the high standard high yield configuration, shown raw (red crosses) and corrected (blue diamonds) for the neutron-induced background scaled up to the N210117 yield (green triangles) (it should be noted that the CR-39 detectors covering the energy range 3–8 MeV were not fielded on N210117).

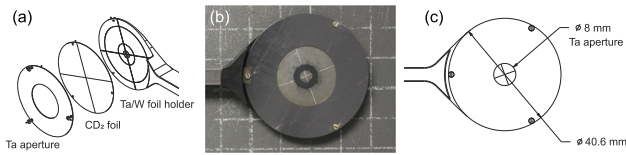


FIG. 4. (a) Cartoon of a 250- μm thick Ta aperture fielded behind the CD foil on the MRS foil holder to reduce the effective foil area, hence instrument efficiency, (b) a picture of the foil assembly from shot N210117, and (c) a new, reduced-size aperture design, which will further reduce the efficiency by a factor of 6.

is to add a rear aperture between the foil and the MRS detector, which is thick enough to range down any deuterons born behind it (Fig. 4). The high yield configuration currently fielded with MRS uses a 3 cm², 250- μm thick Ta rear aperture. A new aperture has been designed and manufactured [Fig. 4(c)] with a 0.5 cm² area, which will reduce the foil effective area and hence MRS efficiency by a factor of 6, bringing the MRS upper yield limit to 2×10^{18} (or 6 MJ).

A promising technique for substantially improving resolution in the MRS measurements at maintained efficiency is fielding a smaller foil closer to the target chamber center (TCC). As discussed in Ref. 10, this works because the ion optical broadening of the signal is much reduced with the smaller MRS foil. On NIF indirect drive implosions, this is achieved by fielding the foil on the hohlraum.⁹ The foils used in this configuration, which are single use by definition, are all made by the GDP method, which conveniently allows them to be deposited directly onto a backer without the use of glue. MCNP and Geant4¹⁸ simulations show that fielding a 0.4 mm diameter, 40- μm thick foil on the hohlraum will improve the resolution by nearly 2 \times compared to standard high yield operation (240 vs 430 keV FWHM) and reduce systematic uncertainty in inferred T_{ion} 4 \times (0.44 vs 0.11 keV) at nearly identical efficiency (4.4×10^{-12} vs 3.8×10^{-12} signal tracks/source neutron). The foil-on-hohlraum technique can also easily be adapted for higher yield by reducing the foil area and thickness and will be required for the next-generation time-resolved neutron spectrometer, MRSt, which is currently under development.^{9,19} However, tests fielding MRS in this configuration undertaken on high-yield NIF implosions N190918, N191007, N200125, N200229, and N200308 identified three issues that must be resolved before this technique becomes broadly applicable. These include (i) interference in the *dsr* region from *n,d* reactions in the hohlraum diagnostic band, (ii) foil movement prior to bang time, and (iii) uncharacterized oxygen content in the foils.

Figure 5 shows MRS data from shots with and without a GDP foil fielded on hohlraums with Al or Cu diagnostic bands. The peak at deuteron energy $E_d \sim 12.5$ MeV is caused by the primary DT neutron peak. The large background structures at $E_d < 8.0$ MeV in the Al band and $E_d < 10.1$ MeV in the Cu band cases do not appear in MRS data with the foil fielded on a foil holder at the standard 26 cm stand-off but arise in the hohlraum case even when MRS is fielded without a foil. Both Al and Cu have non-negligible but poorly characterized cross sections²⁰ for *n,d* reactions; ²⁷Al(*n,d*)²⁶Mg has $\sigma \sim 0.02$ b for 14 MeV neutrons and a Q-value of -6.0 MeV, which is consistent with the upper energy cut-off of 8.0 MeV, and ⁶³Cu(*n,d*)⁶²Ni has

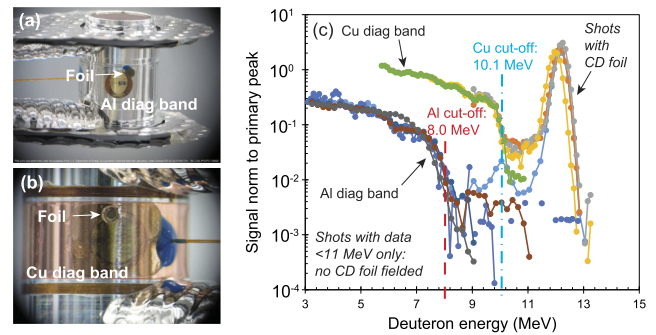


FIG. 5. MRS CD foil fielded on (a) an Al diagnostic band and (b) a Cu diagnostic band hohlraum. In (c), neutron yield-normalized MRS deuteron spectra for both configurations and MRS fielded with and without the CD foil are compared. As indicated by these data, *n,d* reactions in the diagnostic band give rise to a background component, which interferes in the *dsr* region in the Cu case.

$\sigma \sim 0.01$ b and a Q-value of -3.9 MeV, which is consistent with the upper energy cut-off of 10.1 MeV. As a reminder, the E_d scale *dsr* region equivalent is ~ 8.9 – 10.7 MeV, which means this background virtually prevents inference of *dsr* when the foil is fielded on a Cu band hohlraum. A solution to this problem is to always field the MRS foil on a patch of Al or other material that does not generate deuterons in the *dsr* region.

When comparing MRS-measured yield and T_{ion} from these implosions with yields measured by neutron activation detectors²¹ (NAD) and T_{ion} measured with neutron time-of-flight (nTOF) spectrometers,²² MRS yield was found to vary from 75% to 100% of NAD and T_{ion} from 0.4 to 1.5 keV above the average nTOF value. These differences are consistently explained by uncontrolled foil motion prior to burn, randomly ejecting and tilting the foil, reducing efficiency, and increasing resolution compared to nominal. Impact simulations of the hohlraum load confirm that fielding the foil on the edge of a hohlraum diagnostic window makes it susceptible to such motion. These simulations also suggest that this problem can be solved by fielding the foil on an Al tab, which the target fabrication team confirms would be a straightforward modification.

The final GDP foil problem is that this material is known to be susceptible to oxygen uptake,^{23,24} which has not been well characterized. This will impact the MRS resolution; unless corrected for in the response function simulations, it will introduce an error in inferred T_{ion} .¹⁰ Rutherford Backscattering (RBS) experiments using 3 MeV protons generated by the Genesee Pelletron accelerator are underway to characterize the foil impurities, which, if known, can be straightforwardly accounted for in the analysis. Preliminary analysis of the RBS data (Fig. 6) suggests that both nitrogen and oxygen impurities are present in the foils.

IV. REDUCING EFFICIENCY II: FIELDING BEHIND SHIELD WALL

Longer term, higher yields than 2×10^{18} are expected at the NIF, requiring a reduction also of the MRS background. This can be achieved by moving the MRS behind the NIF shield wall (Fig. 1),

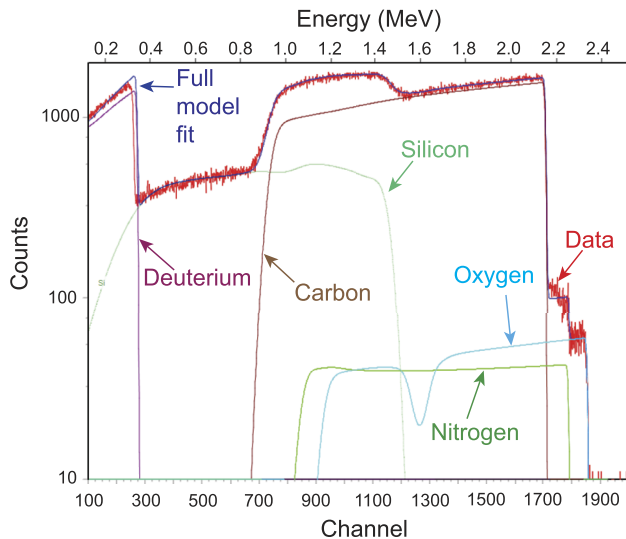


FIG. 6. Result from a Rutherford backscattering experiment of a CD sample deposited onto a Si backer. The data (red) are found to be best described by a full model (dark blue), considering the known Si, C, and D content in the sample and assuming a combination of O (1.4% atomic) and N (1.2% atomic) impurities in the foil.

i.e., moving the magnet aperture from the current 596 to 1866 cm from TCC. Since the signal efficiency scales inversely with distance squared, this results in an $\sim 10\times$ reduction in efficiency. Specifically, efficiency simulations using MCNP with a $50\text{-}\mu\text{m}$ thick, 3 cm^2 active area foil fielded 26 cm from TCC indicate a reduction from 4.4×10^{-12} signal tracks/source neutron in the current location to 4.1×10^{-13} tracks/neutron in the proposed new location. The superiority of the shield wall for reducing neutron-induced background leads to a relatively bigger reduction in neutron-induced background fluence (see Fig. 2), from 2.4×10^{-9} to 4.3×10^{-11} per cm^2 and source neutron in the primary peak; this means the expected S/B improvement is $\sim 5.2\times$. With the previous expected primary overlap limit of 2×10^{18} for the 0.5 cm^2 effective foil area and *dsr* overlap limit of 5×10^{17} due to S/B considerations, the new yield limit for *dsr* can be expected to be $\sim 2 \times 10^{19}$ (or 60 MJ) at maintained S/B. In addition, fielding MRS outside the shield wall is also expected to eliminate the issue of non-uniform background (Fig. 3), further simplifying background subtraction and improving data quality. Such an upgrade would also improve the capability of MRS for measuring low-level features at the high end of the primary DT peak, which can be used to assess the impact of alpha heating in these experiments;²⁵ such a high-level feature is just starting to be discernible above background in the current high-yield configuration on the highest yield shots with $30\times$ yield amplification due to alpha heating.

V. CONCLUSIONS

With the new era of yields of order 1×10^{17} obtained at the NIF, diagnostics need to adapt to continue to provide key measurements to assess implosion performance. In this paper, it is shown that with small modifications, the MRS neutron spectrometer's upper yield limit has been extended to 2×10^{18} for primary (yield and

T_{ion}) measurements and 5×10^{17} for *dsr*. Measurements can also be undertaken at improved resolution by fielding the MRS foil on the hohlraum, provided the hohlraum is modified to eliminate (i) interference in the *dsr* region from diagnostic band *n,d* reactions and (ii) uncontrolled foil motion prior to burn, and provided impurity content in the foils is well characterized. MCNP simulations show that moving the MRS outside the shield wall would allow a further extension of the upper yield limit to 2×10^{19} for both primaries and *dsr* and also facilitate improved measurements of weaker spectral features, including a feature on the high-energy end of the DT peak expected to correlate with alpha heating, at current yields due to a $5.2\times$ improvement in S/B.

ACKNOWLEDGMENTS

This work was supported, in part, by the U.S. Department of Energy NNSA MIT Center-of-Excellence under Contract No. DE-NA0003868 and by Lawrence Livermore National Laboratory under Contract No. B640112. This report was prepared as an account of work sponsored by an agency of the United States Government. Neither the United States Government nor any agency thereof, nor any of their employees, makes any warranty, express or implied, or assumes any legal liability or responsibility for the accuracy, completeness, or usefulness of any information, apparatus, product, or process disclosed, or represents that its use would not infringe privately owned rights. Reference herein to any specific commercial product, process, or service by trade name, trademark, manufacturer, or otherwise does not necessarily constitute or imply its endorsement, recommendation, or favoring by the United States Government or any agency thereof. The views and opinions of the authors expressed herein do not necessarily state or reflect those of the United States Government or any agency thereof.

AUTHOR DECLARATIONS

Conflict of Interest

The authors have no conflicts to disclose.

Author Contributions

M. Gatu Johnson: Conceptualization (equal); Formal analysis (equal); Investigation (equal); Methodology (equal); Software (equal); Writing – original draft (equal). **T. M. Johnson:** Software (equal). **B. J. Lahmann:** Software (equal). **F. H. Séguin:** Funding acquisition (equal); Project administration (equal). **B. Sperry:** Investigation (supporting); Methodology (equal); Software (supporting). **N. Bhandarkar:** Resources (equal). **R. M. Bionta:** Funding acquisition (supporting); Project administration (equal); Supervision (supporting). **E. Casco:** Methodology (equal); Resources (equal). **D. T. Casey:** Project administration (equal); Software (equal); Validation (supporting). **A. J. Mackinnon:** Funding acquisition (equal); Project administration (equal); Resources (equal). **N. Masters:** Conceptualization (supporting); Formal analysis (equal); Software (equal). **A. Moore:** Funding acquisition (equal); Project administration (equal). **A. Nikroo:** Methodology (equal); Resources (equal). **M. Hoppe:** Methodology (equal); Resources (equal). **R. Mohammed:** Methodology (equal); Resources (equal). **W. Sweet:**

Methodology (equal); Resources (equal). **C. Freeman:** Formal analysis (equal); Investigation (equal); Resources (equal); Supervision (equal). **V. Picciotto:** Investigation (equal). **J. Roumell:** Investigation (equal). **J. A. Frenje:** Conceptualization (equal); Funding acquisition (equal); Methodology (equal); Project administration (equal); Supervision (equal); Validation (equal).

DATA AVAILABILITY

The data that support the findings of this study are available from the corresponding author upon reasonable request.

REFERENCES

- ¹A. B. Zylstra *et al.*, *Nature* **601**, 542 (2022).
- ²M. Gatu Johnson *et al.*, *Rev. Sci. Instrum.* **83**, 10D308 (2012).
- ³L. Ballabio, J. Källne, and G. Gorini, *Nucl. Fusion* **38**, 1723 (1998).
- ⁴R. Hatarik *et al.*, *J. Appl. Phys.* **118**, 184502 (2015).
- ⁵M. Gatu Johnson *et al.*, *Rev. Sci. Instrum.* **87**, 11D816 (2016).
- ⁶J. A. Frenje *et al.*, *Nucl. Fusion* **53**, 043014 (2013).
- ⁷J. A. Frenje *et al.*, *Phys. Plasmas* **17**, 056311 (2010).
- ⁸D. T. Casey *et al.*, *Rev. Sci. Instrum.* **84**, 043506 (2013).
- ⁹C. E. Parker *et al.*, *Rev. Sci. Instrum.* **89**, 113508 (2018).
- ¹⁰M. Gatu Johnson *et al.*, *Rev. Sci. Instrum.* **92**, 023503 (2021).
- ¹¹M. Gatu Johnson *et al.*, *Rev. Sci. Instrum.* **85**, 11E104 (2014).
- ¹²A. Zylstra *et al.*, *Nucl. Instrum. Methods Phys. Res. A* **681**, 84 (2012).
- ¹³F. H. Séguin *et al.*, *Rev. Sci. Instrum.* **74**, 975 (2003).
- ¹⁴R. Przewocki *et al.*, *Rev. Sci. Instrum.* **92**, 013504 (2021).
- ¹⁵J. A. Frenje *et al.*, *Rev. Sci. Instrum.* **73**, 2597 (2002).
- ¹⁶MCNP6.2, <https://mcnp.lanl.gov/>, 2017.
- ¹⁷D. T. Casey *et al.*, *Rev. Sci. Instrum.* **82**, 073502 (2011).
- ¹⁸S. Agostinelli *et al.*, *Nucl. Instrum. Methods Phys. Res. A* **506**(3), 250 (2003).
- ¹⁹J. A. Frenje *et al.*, *Rev. Sci. Instrum.* **87**, 11D806 (2016).
- ²⁰See <https://www-nds.iaea.org/exfor/> for a collection of experimentally measured cross section results.
- ²¹D. L. Bleuel *et al.*, *Rev. Sci. Instrum.* **83**, 10D313 (2012).
- ²²T. J. Clancy *et al.*, in *Target Diagnostics Physics and Engineering for Inertial Confinement Fusion III*, edited by P. M. Bell and G. P. Grim (SPIE, Bellingham, 2014), Vol. 9211, SPIE Proc.
- ²³T. R. Gengenbach, Z. R. Vasic, R. C. Chatelier, and H. J. Griesser, *J. Polym. Sci., Part A* **32**, 1399 (1994).
- ²⁴H. Reynolds, S. Baxamusa, S. W. Haan, P. Fitzsimmons, L. Carlson, M. Farrell, A. Nikroo, and B. J. Watson, *J. Appl. Phys.* **119**, 085305 (2016).
- ²⁵J. Källne *et al.*, *Phys. Rev. Lett.* **85**, 1246 (2000).